Available online at www.sciencedirect.com

SCIENCE DIRECT®

Cement and Concrete Research 35 (2005) 731–742

CEMENT AND CONCRETE RESEARCH

Behavior of blended cement mortars exposed to sulfate solutions cycling in relative humidity

M. Nehdi*, M. Hayek

Department of Civil and Environmental Engineering, University of Western Ontario, 1151 Richmond Street, London, Ontario, Canada N6A 5B9

Received 12 June 2003; accepted 20 May 2004

Abstract

In recent years, several cases of damage to concrete structures due to sulfate exposure have occurred essentially in the above ground parts of structures. Such distress, often characterized by white efflorescence and surface scaling, is driven by salt crystallization in pores and/or repeated reconversions of certain sulfates between their anhydrous and hydrated forms under cycling temperature and relative humidity (RH). However, the effect of the water/cementitious materials ratio (w/cm), pozzolanic additions, and other parameters on the durability of cement-based materials under such exposure conditions is still misunderstood. In this study, 12 cement mortars having different w/cm (0.30, 0.45, and 0.60) and made with ordinary portland cement (OPC) or OPC incorporating 8% silica fume, 25% class F fly ash, or 25% blast furnace slag were made. Standard bars from each of these mortars were submerged in both 10% magnesium sulfate ($MgSO_4$) and 10% sodium sulfate (Na_2SO_4) solutions; their expansion and surface degradation was monitored for up to 9 months. In addition, cylinders made from these 12 mortars were partially submerged in 50-mm-deep 10% $MgSO_4$ and 10% Na_2SO_4 solutions. Half of the cylinders were maintained under constant temperature and RH, whereas the others were subjected to cycling RH. The effect of the w/cm and mineral additions on the classic chemical sulfate attack and development of efflorescence was investigated, and the results are discussed in this article.

Keywords: Durability; Sulfate; Expansion; Salt hydration; Efflorescence

1. Introduction

Research on sulfate attack of concrete has flourished in recent years owing to related lawsuits in the United States and Canada. Consequently, the traditional view of sulfate attack has been challenged. For instance, it was suggested that the current testing procedures are not indicative of field conditions and that there is a need for the development of failure criteria and parameters that can enable the predicting of sulfate attack in field structures [1]. A critical analysis of sulfate attack mechanisms, related test techniques, field monitoring methods, and development of pertinent modeling criteria was recently presented [2]. The controversies and confusion caused by existing literature lead Mehta [3] to present a critical examination of the state-of-the-art research information on this subject. Skalny et al. [4] recently published a comprehensive review on sulfate attack in concrete.

There has been growing emphasis of recent research in this area on the distinction between chemical and physical types of sulfate attack. In the so-called chemical attack, the sulfate ions (SO_4^{2-}) enter in reactions with cement hydration products leading primarily to the formation of ettringite and gypsum. However, ongoing controversy exists as to what is the effect of each of these products on the deterioration of concrete. Researchers have often focused on the effect of the SO_4^{2-} without equal attention to the cations associated with them (Ca, Na, Mg, and Fe). It is now known that low tricalcium aluminate (C_3A) cements, which are considered resistant to sodium sulfate (Na_2SO_4) attack, can be detrimental in exposure conditions involving magnesium sulfate ($MgSO_4$) or sulfuric acid [2], because the prevailing low pH conditions are conducive to direct attack on the calcium silicate hydrates (CSH).

Formation of ettringite and subsequent expansion and cracking have often been invoked as the driving mechanisms of chemical sulfate attack [5–7]. At high SO_4^{2-} concentrations and/or with gradual decrease of pH, ettringite is not stable and decomposes to form gypsum. Yet, the

* Corresponding author. Tel.: +1-519-661-2111x88308; fax: +1-519-661-3779.

E-mail address: mnehdi@eng.uwo.ca (M. Nehdi).

0008-8846/$ – see front matter © 2004 Elsevier Ltd. All rights reserved.
doi:10.1016/j.cemconres.2004.05.032

nature of disruption caused by gypsum is not well understood. During this process, the buffering calcium cations are depleted and decalcification of CSH begins, leading to softening and loss of mass [3], which are two distress mechanisms commonly observed in field cases of sulfate attack. Such a scenario is especially prevalent under $MgSO_4$ exposure in which a layer of brucite is typically formed on the surface of concrete ultimately depleting calcium hydroxide (CaOH) and lowering the pH. This prompts the CSH to release more CaOH to the surrounding solution in an attempt to raise the pH and remain stable, which eventually contributes to the decalcification of CSH and the formation of noncementitious magnesium silicate hydrate [8].

However, sulfate-induced degradation has also been reported in cases where ettringite and gypsum that are characteristic of chemical sulfate attack were not found in the deteriorated concrete [9]. This type of attack is physical whereby salt-bearing solutions rise in concrete by capillarity. After surface evaporation, the solution becomes supersaturated, leading to salt crystallization in the pores of concrete, therefore generating pressures that can cause cracking.

Literature on salt weathering of building stone and brick from as early as 1864 (discussed elsewhere; Refs. [10–13]) points out to another mechanism of sulfate attack. Within daily environmental changes in many areas of the world, certain salts [e.g., Na_2SO_4 and sodium carbonate] can cycle between their hydrated and anhydrous forms. For instance, the conversion of anhydrous Na_2SO_4 (thenardite) to decahydrate (mirabilite) involves an expansion of around 315% [12]. In this case, it may not be the crystallization pressure of salt but the cumulative effect of pressures due to thenardite–mirabilite conversion that causes the deterioration of concrete, a mechanism coined as salt hydration distress by Hime et al. [12]. However, research by Rodriguez-Navarro and Doehne [11] suggest that this should be reconsidered. Contrary to the view that salt hydration pressure in a porous material is the source of physical damage, their results obtained on field environmental scanning electron microscopic (SEM) observations of salt crystallization events rather suggest that crystallization of thenardite in pores may be the source of most of the physical damage.

Because experience shows that salt weathering was more severe in rocks with finer pores, there is a concern that concrete with lower water/cementitious materials ratio (w/cm) and/or incorporating pozzolanic additions could be more vulnerable to this physical type of salt distress; indeed, such a trend was reported by Hime [14]. The implication is that good-quality durable concrete may not be so durable when it comes to salt weathering. Therefore, in this study, mortars with low, moderate, and high w/cm (0.30, 0.45, 0.60) and made with plain ordinary portland cement (OPC) and OPC incorporating 8% silica fume, 25% slag, or 25% class F fly ash were made. They were tested with both Na_2SO_4 and $MgSO_4$ solutions in fully submerged conditions and in partially submerged conditions under constant and cycling relative humidity (RH). The results should highlight the effect of the w/cm and pozzolanic additions on the resistance of the mortars to conventional chemical sulfate attack versus their resistance to physical salt weathering.

2. Materials

A type 10 Canadian cement (CSA3-A5-M93) similar to ASTM type I cement was used to make the various mortar mixtures. In addition, silica fume, class F fly ash, and ground granulated blast furnace slag were used as supplementary cementitious materials. Table 1 summarizes the physical and chemical properties of the various binders. Standard Ottawa sand (ASTM C778-91 Standard Specification for Standard Sand) was used to prepare the mortars. To achieve similar flow (115 ± 5%) on a standard flow table (ASTM C230-90 Specifications for Flow Table for Use in Tests of Hydraulic Cement) for all mortars and therefore eliminate the effect of workability on results, a naphthalene sulfonated superplasticizer having 42% solid content was used at different dosages in some of the mixtures.

Table 1
Physical and chemical properties of type 10 portland cement and pozzolanic additions

Properties	Type 10 cement	Class F fly ash	Slag	Silica fume
Silicon oxide (SiO_2)	19.5	48.9	34.8	94.0
Aluminum oxide (Al_2O_3)	5.2	23.3	9.8	0.1
Ferric oxide (Fe_2O_3)	2.4	14.9	0.6	0.1
Calcium oxide (CaO)	61.3	3.8	38.3	0.4
Magnesium oxide (MgO)	2.5	0.7	9.6	0.4
Sodium oxide (Na_2O)	0.3	0.6	0.4	0.1
Potassium oxide (K_2O)	1.2	1.7	0.4	0.9
Equivalent alkali ($Na_2O + 0.658\ K_2O$)	0.8	0.4	0.7	0.7
Phosphorous oxide (P_2O_5)	0.1	–	–	< 0.01
Titanium oxide (TiO_2)	0.3	–	0.8	0.3
Sulfur trioxide (SO_3)	4.1	0.2	3.5	1.3
Loss on ignition	2.8	0.3	–	2.7
Specific surface area (m^2/kg)	412	280	468	24,940
Mean particle size (laser diffraction; μm)	13.53	16.56	12.60	0.16
Specific gravity	3.17	2.08	2.90	2.02
Tricalcium silicate (C_3S)	51.1			
Dicalcium silicate (C_2S)	17.4			
Tricalcium aluminate (C_3A)	9.7			
Tetracalcium aluminoferrite (C_4AF)	7.4			
Initial setting, Vicat test (min)	180			
Final setting, Vicat test (min)	350			
$f'c$ of standard cube (MPa) 7 days	32.1			
$f'c$ of standard cube (MPa) 28 days	38.8			

3. Experimental program

Four different binders were used in this study: 100% OPC, 92% OPC-8% silica fume, 75% OPC-25% class F fly ash, and 75% OPC-25% blast furnace slag. For each binder, three different mortar mixtures at a w/cm of 0.30, 0.45, and 0.60 were prepared according to ASTM C305-82 (Practice for Mechanical Mixing of Hydraulic Cement Pastes and Mortars of Plastic Consistency). In each of the resulting 12 mortar mixtures, the sand/binder mass ratio was maintained equal to 2.75, and the flow table value was maintained at 115 ± 5%. For each mixture, 12 cylinders (50 × 100 mm) were made to monitor the development of compressive strength, 16 bars (25 × 25 × 285 mm) were made for the ASTM C1012 sulfate expansion test, and 6 cylinders (100 × 200 mm) were prepared for the salt hydration test. All specimens were covered with plastic sheets and wet burlap for the first 24 h. After demolding, all specimens were stored in a curing chamber at 23 ± 1.7 °C and RH>95% until they reached a compressive strength of 20.0 ± 1.0 MPa. Eight bar specimens from each mixture were then submerged in a Na_2SO_4 solution (10% by mass of Na_2SO_4), and another eight bars were submerged in a $MgSO_4$ solution (10% by mass of $MgSO_4$). The containers in which the bars were immersed were made of plastic, and a means for supporting the bars was included so that no end or side of a bar specimen rested against the container. The pH value of the sulfate solutions was maintained in the range of 6–8 by replacing the solution with a fresh one when needed. Before placing the bar specimens in the sulfate solutions, their length was measured using a high-accuracy digital length comparator. The length change of the specimens was then monitored at 1, 2, 3, 4, 8, 13, and 15 weeks after they were placed in the sulfate solutions. If slight, gradual, and uniform length change was taking place, the next measurements were made at 4, 6, and 9 months. When expansion was occurring rapidly at any stage of the test, the interval between readings was adequately shortened.

In addition, when the mortar specimens reached 20.0 ± 1.0 MPa, the 100 × 200 mm cylinders were removed from the curing room and stored indoors for 60 days under laboratory conditions. Each cylinder was cut along its diameter into two half cylinders using a dry diamond saw cut. From each of the 12 mortar mixtures, two half cylinders were submerged in a 50-mm-deep 10% Na_2SO_4 solution, whereas the other two half cylinders were submerged in a 50-mm-deep 10% $MgSO_4$ solution. In each sulfate solution bath, half-cylinder specimens, which were made from the same binder but at three different w/cm, were tested side by side to visually compare the effect of the w/cm on salt hydration effects. Replicates from each half-cylinder specimen were tested to verify reproducibility of results: two in a Na_2SO_4 solution at a constant RH of 32 ± 3%, two in a similar solution that is cycling in RH between >95% and 32 ± 3%, two specimens in a $MgSO_4$ solution at constant RH of 32 ± 3%, and two specimens tested in a $MgSO_4$ solution cycling in RH between >95% and 32 ± 3%. RH cycling consisted of consecutive sequences of 24 h at RH>95% followed by 24 h at RH of 32 ± 3%. The height of capillary rise of the sulfate solutions was monitored for all specimens, and a digital camera was used to record the status of white efflorescence forming on the various specimens at various time periods. Moreover, at the same age when half-cylinder specimens were partially submerged in Na_2SO_4 and $MgSO_4$ solutions, small specimens (20 mm in diameter) were taken using a core drill from 100 × 200 mm cylinder specimens. After vacuum drying, their porosity was evaluated using nitrogen adsorption and mercury intrusion. The goal is to examine whether the formation of efflorescence is affected by the porosity of the mortar specimens. The resulting efflorescence on specimens was analyzed using X-ray diffraction, SEM imaging, and X-ray elemental analysis.

4. Analysis of results

4.1. Expansion in Na_2SO_4

Fig. 1a illustrates the expansion after 9 months of immersion in a 10% Na_2SO_4 solution of mortar bars having

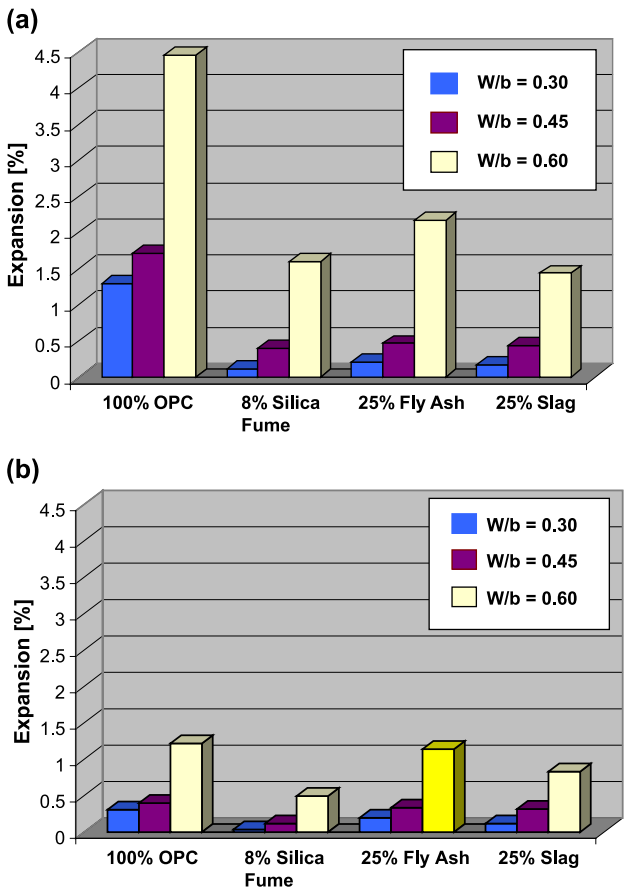

Fig. 1. Average expansion of mortar bars after 9 months of immersion in (a) 10% Na_2SO_4 solution and (b) 10% $MgSO_4$ solution.

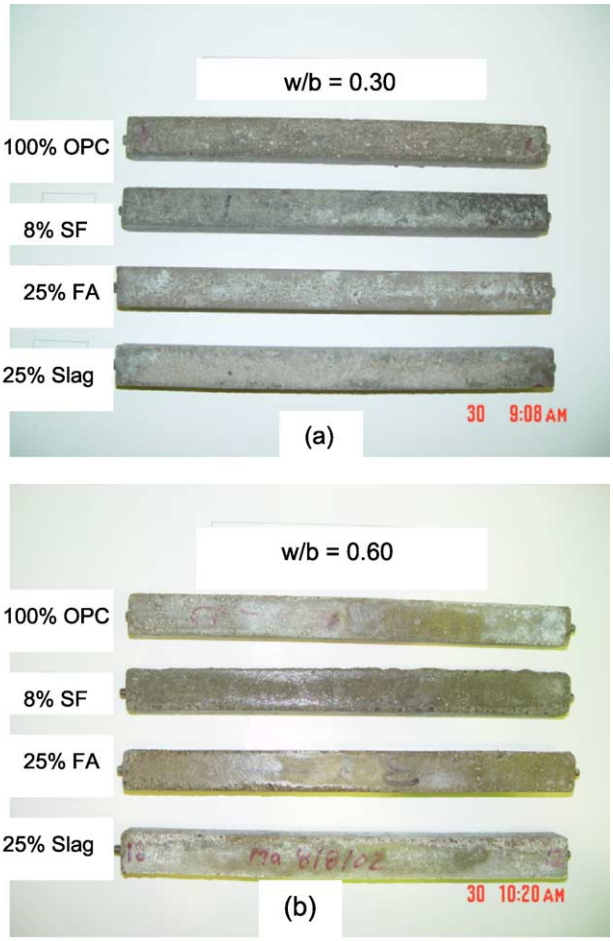

Fig. 2. Surface degradation of bar specimens submerged for 9 months in a 10% $MgSO_4$ solution (a) at w/b ratio of 0.30 with mixtures incorporating pozzolanic additions showing better performance than that of OPC specimens and (b) at w/b ratio of 0.60 with mixtures incorporating pozzolanic additions showing lower performance than that of OPC specimens.

different w/cm and incorporating various mineral additions. The results confirm what is already known: the higher the w/cm, the higher the expansion for all 12 mortar mixtures. Increasing the w/cm from 0.45 to 0.60 increased expansion much more significantly than when it was increased from 0.30 to 0.45. Moreover, the plain OPC mortar had the highest sulfate expansion. The addition of 8% silica fume achieved the highest reduction in sulfate expansion followed by the 25% slag and 25% class F fly ash, respectively. At a high w/cm of 0.60, 25% slag was somewhat more effective in controlling expansion than 8% silica fume.

4.2. Expansion in $MgSO_4$

Fig. 1b shows the expansion of mortar bars identical to those discussed above but submerged in a 10% $MgSO_4$ solution. The data exhibit a similar trend to that observed in immersion in Na_2SO_4: the higher the w/cm, the higher the expansion for all 12 mortar mixtures, and pozzolanic mineral admixtures tended to decrease expansion, with 8% silica fume being the most effective followed by 25% slag and 25% class F fly ash, respectively. It is worth noting that the expansion values reached under Na_2SO_4 immersion were significantly higher than those reached under $MgSO_4$ immersion.

4.3. Surface degradation of mortar specimens

Surface deterioration was not clearly identifiable on the mortar bars immersed in the 10% Na_2SO_4 solution. However, surface scaling and loss of mass could be identified on the mortar bars immersed in the 10% $MgSO_4$ solution, and this effect seemed to increase with time of exposure (Fig. 2). While pozzolanic admixtures tended to significantly reduce expansion due to sulfate exposure, in both sodium and magnesium solutions, such a beneficial effect was not achieved with regards to $MgSO_4$ surface degradation. In fact, the 8% silica fume mortar bars had surface degradation similar to or somewhat better than that of the control OPC bars at low and moderate w/cm, whereas they had more surface degradation at high w/cm. It seems that,

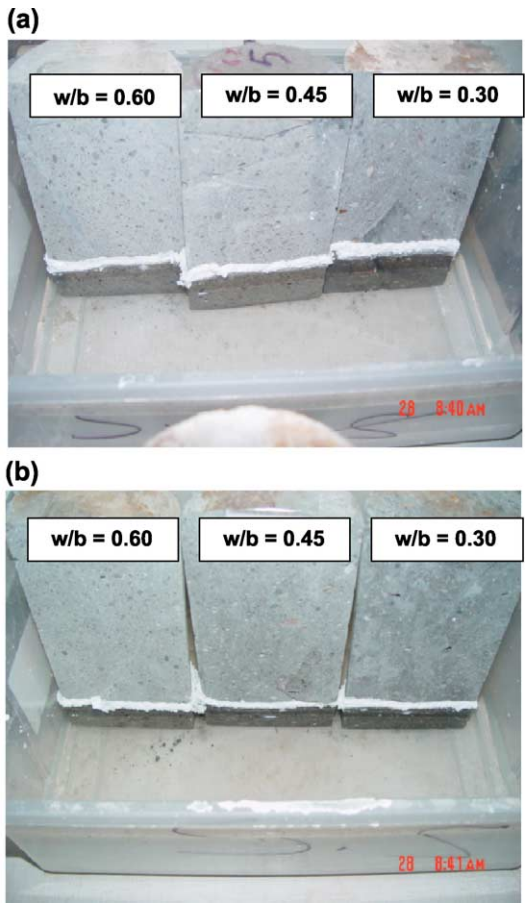

Fig. 3. Example of mortar half cylinders with different w/b ratio and incorporating (a) 100% OPC and (b) 8% silica fume after 167 h of partial submersion in a 50-mm-deep 10% Na_2SO_4 solution at constant RH = 32 ± 3%.

because silica fume consumes CaOH, it lowers the pH, allowing the magnesium surface attack and decalcification of CSH to proceed more rapidly. In the low w/cm mortar bars, this effect was offset by the reduced permeability imparted by silica fume, but in the high w/cm mortars, permeability was high and the detrimental effect was dominant. A similar trend can be observed for the class F fly ash mortar specimens. Only slag mortar specimens seemed to have slightly improved resistance to surface attack by $MgSO_4$ probably because the calcium-rich slag did not reduce the pH as much as silica fume and class F fly ash did. Similar trends of results were reported by other researchers [15,16].

4.4. Salt hydration

4.4.1. Na_2SO_4 solution at constant RH

Fig. 3a and b illustrate an example of mortar half cylinders having different w/cm after 167 h of partial immersion in a 50-mm-deep 10% Na_2SO_4 solution at a constant RH of $32 \pm 3\%$. The same Na_2SO_4 solution was divided in four plastic containers, and in each container, half cylinders made with w/cm of 0.30, 0.45, and 0.60 for each of the four different binders mentioned above were tested side by side. It was observed that capillary rise of the sodium solution was limited in all cylinders and that the effect of the w/cm was not significant. A thin layer of white efflorescence formed just above the solution line for all specimens and was somewhat thicker in the fly ash and slag specimens.

4.4.2. Na_2SO_4 solution at cycling RH

Fig. 4a–d illustrate mortar half cylinders made with plain OPC, 8% silica fume, 25% fly ash, and 25% slag, respectively, and having w/cm of 0.30, 0.45, and 0.60 after 151 h of partial immersion in a 50-mm-deep 10% Na_2SO_4 solution cycling in RH between $32 \pm 3\%$ and >95%. For all half cylinders, white efflorescence started to form at the first low RH cycle and kept increasing in height and thickness during subsequent cycles. It can be noted that the 8% silica fume specimens were somewhat more affected followed by the 25% slag, 100% OPC, and 25% fly ash specimens, respectively. Generally, specimens having an

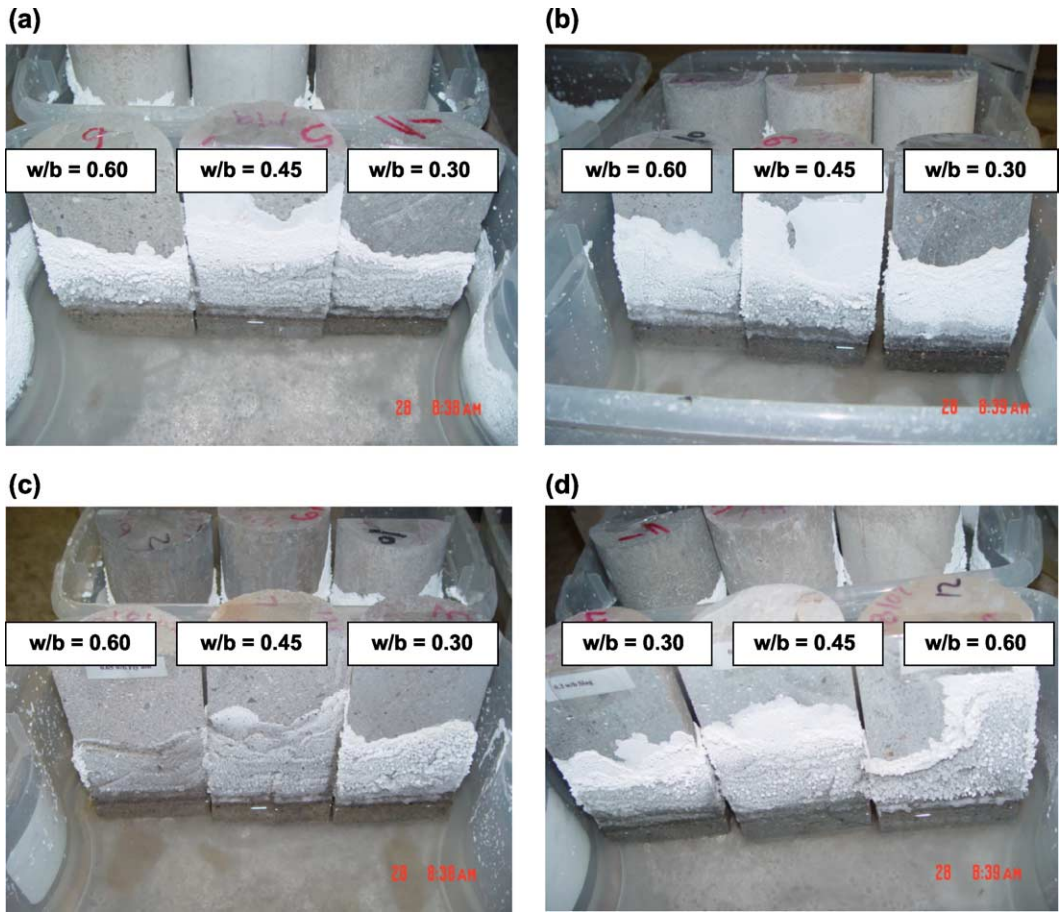

Fig. 4. Mortar half cylinders with different w/b ratio and incorporating various pozzolanic additions after 151 h of partial submersion in a 50-mm-deep 10% Na_2SO_4 solution cycling between RH = $32 \pm 3\%$ and RH>95%. (a) 100% OPC mortar partially immersed in Na_2SO_4 after 151 h from end of first RH cycle. (b) 8% Silica fume mortar partially immersed in Na_2SO_4 after 151 h from end of first RH cycle. (c) 25% Fly ash partially immersed in Na_2SO_4 after 151 h from end of first RH cycle. (d) 25% Slag partially immersed in Na_2SO_4 after 151 h from end of first RH cycle.

intermediate w/cm of 0.45 had the most extensive efflorescence, whereas those with a w/cm of 0.60 and 0.30 had a comparable behavior.

4.4.3. $MgSO_4$ solution at constant and cycling RH

Fig. 5 shows half-cylinder mortar specimens made with pure OPC, 8% silica fume, 25% fly ash, and 25% slag, respectively, and having w/cm of 0.30, 0.45, and 0.60 after 151 h of partial immersion in a 50-mm-deep 10% $MgSO_4$ solution at RH cycling between 32 ± 3% and >95%. Similar to the case where RH was constant, there was no formation of efflorescence. The effects of variation of the w/cm and type of binder were both not significant. Unlike Na_2SO_4, $MgSO_4$ is not known to have hydrated and anhydrous forms, which explains the observed behavior.

4.5. Effect of water/binder ratio and pozzolanic additions on salt hydration

The observation that rocks with finer pore structure were more vulnerable in field conditions to salt weathering lead to the controversial suggestion that concrete with lower w/cm or incorporating mineral additions known to refine its pore structure would also be more vulnerable to salt crystallization/hydration distress. To examine this aspect, Fig. 6 illustrates mortar half cylinders made with pure OPC and 8% silica fume at w/cm of 0.30, 0.45, and 0.60. In each case, half cylinders partially submerged in a 50-mm-deep 10% Na_2SO_4 solution for 167 h under constant RH and for 151 h under cycling RH were placed side by side for visual comparison. It can be seen that the half cylinders made with an intermediate w/cm of 0.45 were the most affected by efflorescence, and specimens made with silica fume were somewhat more affected than those made with pure OPC. It is recommended that research monitoring possible degradation of mortar/concrete resulting from such efflorescence under long-term field exposure be conducted to investigate the effect of the w/cm and mineral additions more thoroughly.

4.6. X-ray diffraction and SEM analysis of efflorescence

Fig. 7 shows a typical X-ray diffractogram of efflorescence developed on half cylinders cycling in RH and

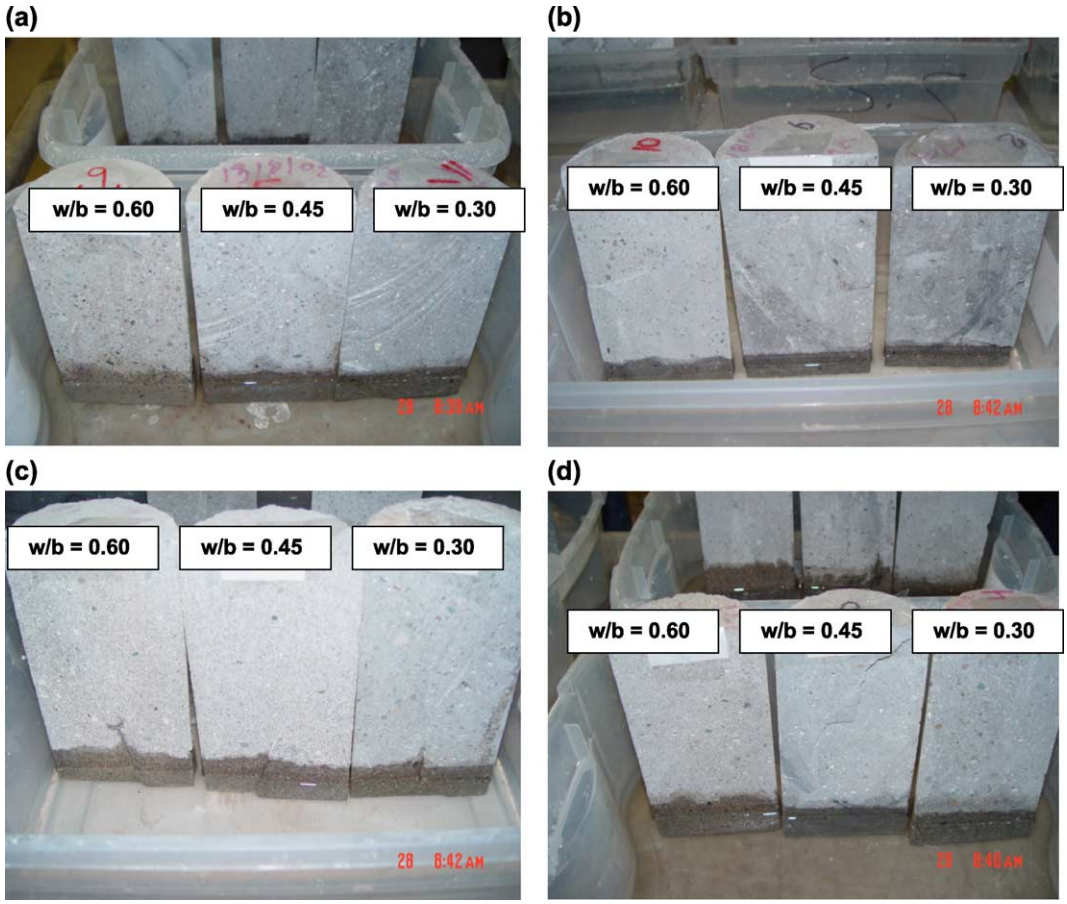

Fig. 5. Mortar half cylinders with different w/b ratio and incorporating various pozzolanic additions after 151 h of partial submersion in a 50-mm-deep 10% $MgSO_4$ solution cycling between RH = 32 ± 3% and RH>95%. (a) OPC mortar partially immersed in $MgSO_4$ after 151 h from end of first RH cycle. (b) 8% Silica fume mortar partially immersed in $MgSO_4$ after 151 h from end of first RH cycle. (c) 25% Fly ash mortar partially immersed in $MgSO_4$ after 151 h from end of first RH cycle. (d) 25% Slag mortar partially immersed in $MgSO_4$ after 151 h from end of first RH cycle.

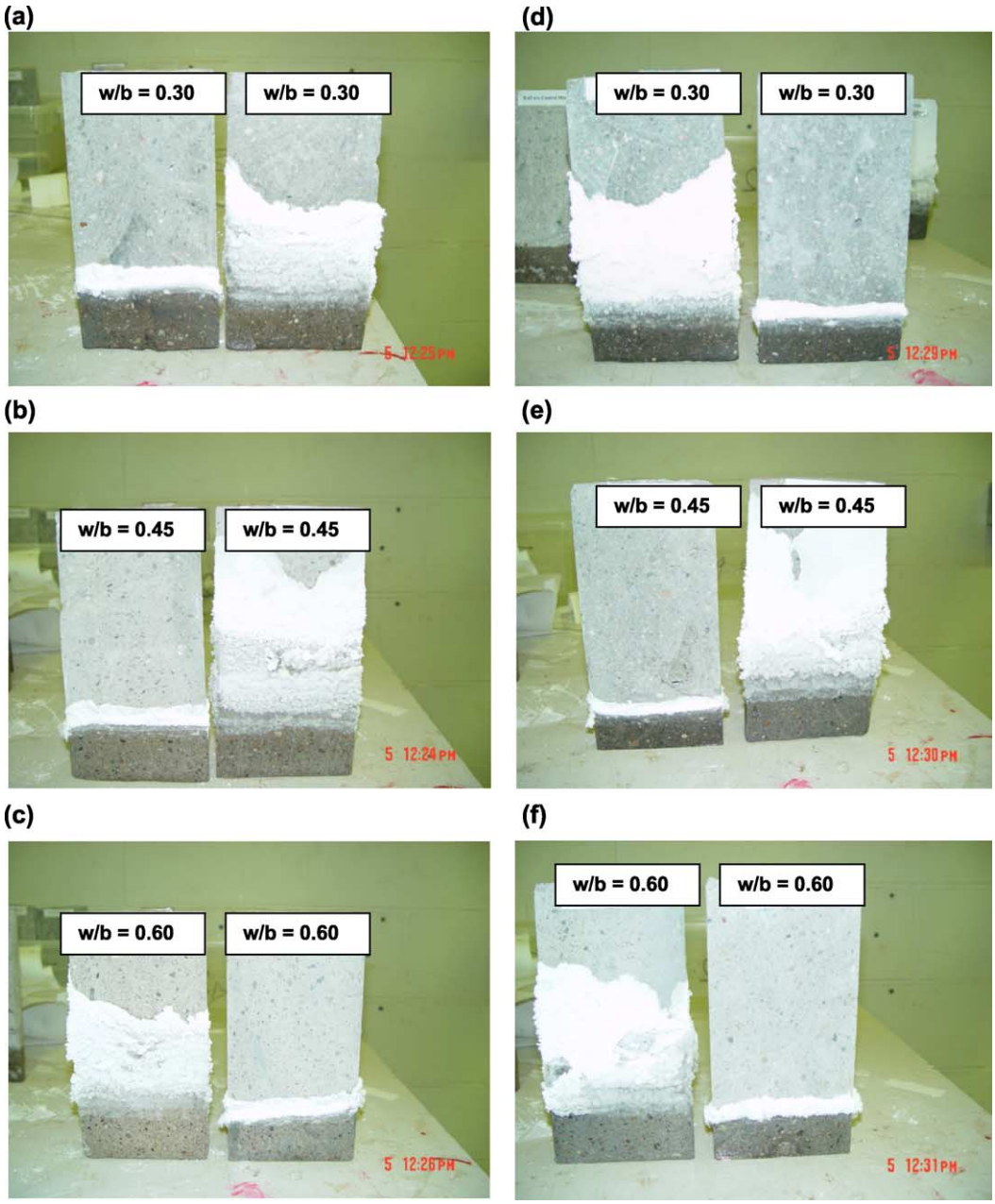

Fig. 6. Effect of w/b ratio and silica fume addition on salt hydration. (a) 100% OPC mortar, w/c = 0.30, in Na_2SO_4, at constant RH (left) and cycling RH (right). (b) 100% OPC mortar, w/c = 0.45, in Na_2SO_4, at constant RH (left) and cycling RH (right). (c) 100% OPC mortar, w/c = 0.60, in Na_2SO_4, at constant RH (right) and cycling RH (left). (d) 8% Silica fume mortar, w/b = 0.30, in Na_2SO_4, at constant RH (right) and cycling RH (left). (e) 8% Silica fume mortar, w/b = 0.45, in Na_2SO_4, at constant RH (left) and cycling RH (right). (f) 8% Silica fume mortar, w/b = 0.60, in Na_2SO_4, at constant RH (right) and cycling RH (left).

partially submerged in a 10% Na_2SO_4 solution. X-ray tests were conducted in a Rigaku RTP 300RC rotating anode diffractometer with CuK_α radiation (10° per minute at 160 mA, 45 kV). The peaks in the diffractogram match the thenardite card 37-1465 in the JCPDS databases, with traces of mirabilite (card 11-647). Fig. 8 shows SEM images of the efflorescence at different magnifications. Typical thenardite crystals are abundant with limited occurrence of mirabilite crystals. Elemental X-ray analysis (Fig. 8d) identified the components of Na_2SO_4, with traces of gold from the coating used in sample preparation.

5. Discussion

5.1. W/cm, hydration, permeability, and sulfate-induced expansion

As per the ASTM C1012 requirements, the exposure of the various mortar specimens to submersion in Na_2SO_4 and $MgSO_4$ solutions started when their compressive strength reached 20 MPa. Similar strength at the onset of sulfate exposure provides a basis for comparing the performance of the various specimens. However, mercury

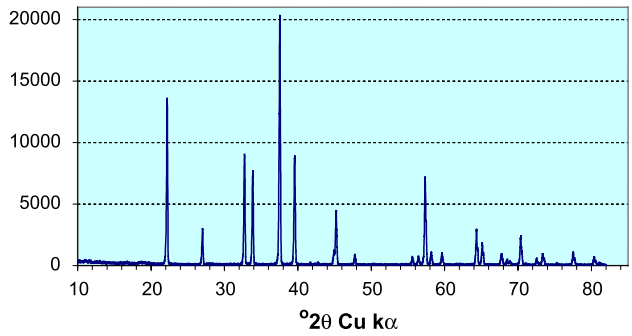

Fig. 7. Typical X-ray diffractogram of efflorescence showing pattern of thenardite with traces of mirabilite.

intrusion and nitrogen adsorption results showed that, for the three w/cm used, this strength corresponds to very different levels of hydration and, therefore, different pore size distributions and total porosities. The other alternative is to start sulfate exposure for all specimens based on the same degree of hydration. In addition to making the test too complicated, this also would not ensure that the specimens have the same permeability, let alone similar pore size distributions. Furthermore, in field conditions, there is no such grace period that is provided before contact between the concrete and sulfate-bearing solutions. Depending on exposure conditions such as the level of the underground water table, ingress of sulfates in the pore system of concrete can start at very early ages or after an advanced level of hydration. Nevertheless, expansion tests in this study confirmed what we already know that making good-quality concrete with low w/cm and assuring good compaction and curing to reduce permeability can reduce expansion, which is essential for durability of concrete in sulfate environments. The effect of the w/cm on efflorescence involves different mechanisms and will be discussed later.

5.2. Supplementary cementitious materials and expansion

It can also be argued that the benefits of supplementary cementitious materials, especially those with slow reactivity, are mostly realized in mature specimens at higher degree of hydration. However, laboratory expansion is usually monitored up to 9 months of exposure and beyond, which involves the behavior of binders at higher levels of hydration. Still, the kinetics of hydration vary in different binder systems. It would not be advisable to test specimens at a mature age, and when good performance is observed,

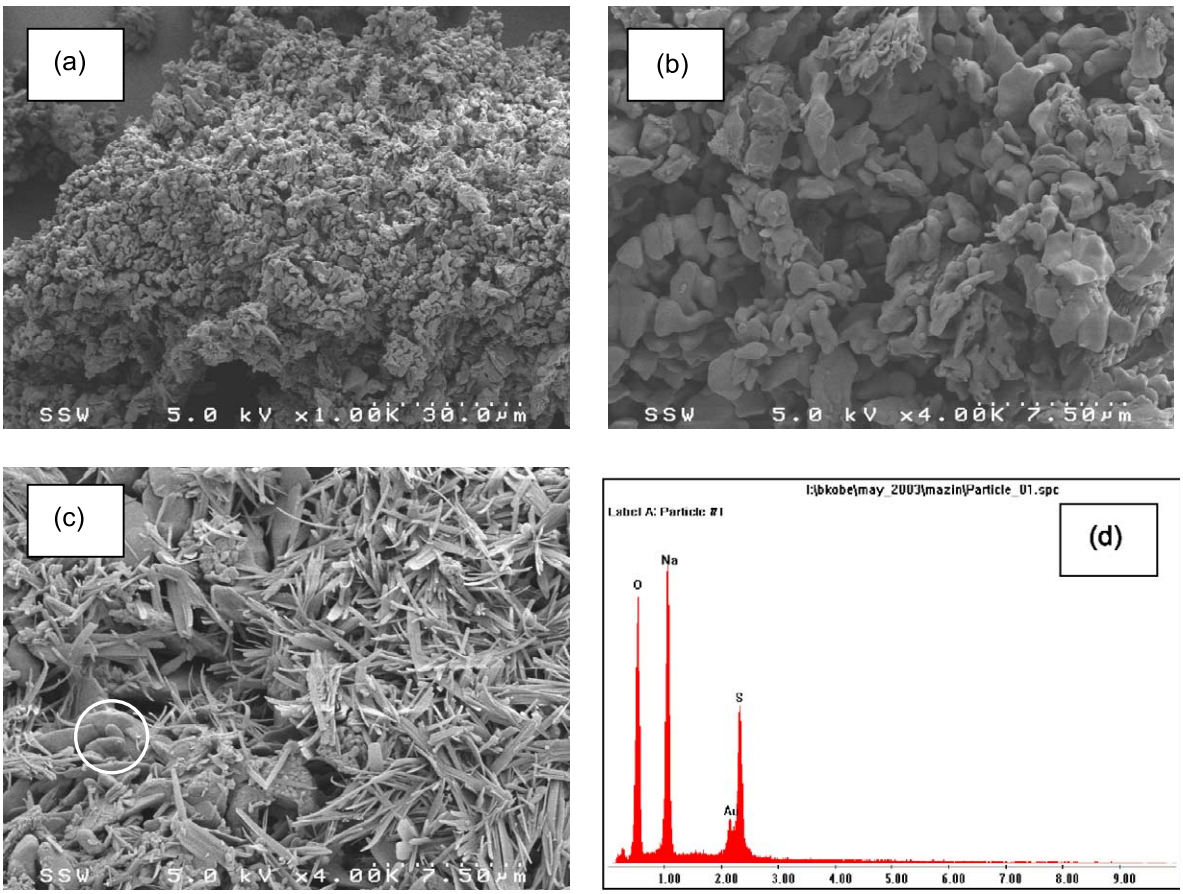

Fig. 8. Illustration of thenardite at (a) 1000 × and (b) 4000 × , (c) coexistence of thenardite and mirabilite, and (d) X-ray elemental analysis of circled area in (c) showing components of Na_2SO_4 and traces of gold from sample preparation.

recommend the use of corresponding mixture designs for use in aggressive sulfate environments. In field conditions, the mechanisms of sulfate attack do not wait for concrete to mature to start acting on it. However, laboratory results usually overestimate damage from sulfate exposure due to higher sulfate concentrations used in laboratory tests, size effects that make damage more severe in small-dimension high surface/volume ratio specimens, and ignoring the effect of other ions present in field sulfate solutions that affect transport mechanisms [17].

Results of this study show that silica fume, fly ash, and slag reduced Na_2SO_4 expansion. This is believed to be due to reduced permeability through pozzolanic reactions that consume CaOH to produce more CSH. In addition, cement replacement reduces the overall amount of C_3A in the system and, consequently, the amount of ettringite and gypsum that can form upon sulfate attack. However, for such benefits to be achieved, adequate curing is needed. In $MgSO_4$, the reduced free CaOH due to pozzolanic reactions and resulting low pH initiate the decomposition of CSH earlier than in OPC systems through the release of more CaOH. The released CaOH is immediately converted to magnesium hydroxide [$Mg(OH)_2$] and calcium sulfate ($CaSO_4$) leading to further release of CaOH and eventually severe degradation of CSH. Thus, supplementary cementitious materials do not seem to significantly enhance durability under $MgSO_4$ attack. Nevertheless, in regions that are distant from the front of precipitation of magnesium oxide (MgO)-bearing compounds, the pH is still high and SO_4^{2-} migrating inward can still form ettringite by reacting with monosulfate and portlandite. This is likely the reason why there is some expansion occurring in specimens submerged in $MgSO_4$ and why supplementary cementing materials appear to reduce such expansion through mechanisms similar to those explained earlier for Na_2SO_4. However, such benefits are of little practical relevance because, unlike the attack by alkali sulfates that cause damage through expansion, $MgSO_4$ attack is characterized essentially by loss of strength and disintegration of cohesive properties.

5.3. Mechanisms of expansion

Because reactions of cementitious systems in which SO_4^{2-} are involved are rather associated with chemical shrinkage, expansion of concrete due to sulfate exposure is not intuitively clear. Types of expansive reactions and related mechanisms for cement-based materials have been proposed by various researchers; they are discussed in detail by Skalny et al. [4]. These include increase of solid volume, expansion in topochemical reactions, oriented crystal growth, expansion due to crystallization pressure, expansion due to swelling processes, and other phenomena. The majority of investigators suggest that topochemical ettringite formation around its precursors and its oriented growth are the major cause of expansion in sulfate-calcium-aluminate systems [4]. In topochemical reactions, the product of the reaction must form within the space of one of the reactants, often through crystalline overgrowth on it. It is not immediately clear then why a higher w/c ratio appears to lead to higher expansion. Not only higher w/c ratio makes through solution reactions and long-range diffusion of hydration products more likely (which is against the assumption of topochemical reaction), but it also makes the size of pores larger. It is generally believed that pressure due to crystal growth is lower in larger pores (for instance, Ref. [18]). Furthermore, expansion would not occur until the pore space is filled with the precipitating phase so that newly deposited material exerts pressure on the already deposited. Intuitively, a high w/cm increases the pore space and would delay the onset of such expansion. We propose herein that various mechanisms combine to make sulfate-induced expansion higher the higher the w/c ratio. First, the higher permeability of the system ensures that a larger volume of a concrete element is affected by sulfate ingress and contributes to expansion. In addition, in low w/cm systems, the precipitated ettringite and gypsum tend to block the path for further ingress of sulfates due the initially low porosity. In addition, due to high pore connectivity of high w/cm systems, pore pressure is transferred through the liquid phase to longer distances, and eventually, pressures generating in various pores can join effects to produce higher expansions.

It is known that, for topochemical formation of ettringite to occur, the liquid phase must contain sufficiently high concentrations of CaOH (various references reported in Ref. [4]). At such high concentrations, aluminate ions cannot migrate too far from the phase serving as a precursor to ettringite formation, which supports topochemical growth of ettringite on aluminate phases. It is suggested herein that this mechanism could also be an additional reason why supplementary cementitious materials tend to decrease expansion. The low concentrations of CaOH in the liquid phase due to the pozzolanic reaction lead to random and less localized precipitation of ettringite from the liquid phase (no oriented growth takes place), which results in decreased expansion. This also explains why highly reactive pozzolanic materials such as silica fume tend to be most efficient in controlling sulfate expansion, whereas decreasing permeability through reduction of the w/c ratio does not achieve as drastic expansion reduction results. It could also explain why class F fly ash that tends to decrease CaOH in the pore solution more than class C fly ash is also much more effective than the latter in combating sulfate-induced expansion in concrete.

5.4. Salt crystallization and efflorescence

Field experience in areas of the world with sulfate-rich groundwater indicates the rarity of serious degradation of concrete due to classic ettringite and gypsum related expansion. Instead, surface scaling in the above ground part of

structures (mainly foundations) was the common form of degradation. Apparently, this surface scaling is caused by stresses from expansion associated with formation of ettringite and/or crystallization pressure when gypsum precipitates [in low aluminum oxide (Al_2O_3) systems or at low pH] in the underlying surface layer [19]. Haynes [17] suggests that the progressive lowering of pH from the surface of concrete inward would cause the decomposition of ettringite into gypsum and other compounds. The gypsum formation near the concrete surface can cause exfoliation of the surface. However, earlier in the same article, Haynes reports that petrographers across the United States have examined hundreds of concrete cores from foundations of houses involved in sulfate attack litigations in California, only to find that, in rare instances, there was gypsum in minor amounts within the exterior 5 mm of the concrete surface, whereas there was no major signs of expansion-induced sulfate attack.

In the presence of a drying front, for instance, when water can evaporate from the surface of concrete, and with high concentrations of alkali sulfates such as in the present study, crystallization of salts can occur. If the drying front is at the concrete surface (supply of sulfate solution is high, evaporation rate is low), then this can result in simple deposition of salts at the surface in the form of efflorescence. This does not imply that expansive reactions and/or decalcification of the cementitious matrix are not simultaneously taking place. However, if the drying front moves inward inside the concrete surface layer (higher evaporation rate than supply of sulfate solution), then salts can crystallize in the concrete pores from the supersaturated solution, resulting in disruptive pressures [18,19]. Furthermore, for Na_2SO_4 and in the presence of cycling temperature and/or RH, it can readily cycle between hydrated (mirabilite) and unhydrated (thenardite) forms, with associated changes in volume of ~ 315% (it should be noted that change from mirabilite to thenardite and vice versa can occur at constant RH and cycling temperature, at constant temperature and cycling RH, or at simultaneous changes of temperature and RH). This repeated volume change results in fatigue adding to pressure crystallization to cause surface scaling of concrete. This latter mechanism is at times called a new degradation process, whereas literature on building stone and brick indicates that the phenomenon has been known for decades (e.g., [9–11,13]).

The issue of sulfate-related efflorescence and salt crystallization is, however, controversial. First, there is no agreement on whether such process is chemical or physical. Haynes et al. [20] stress that salt crystallization is a physical mechanism distinct from chemical sulfate attack. Apparently, crystal formation is a chemical feature with physical consequences, and sulfate attack may be a system of complex physiochemical processes acting in a synergistic scheme. Thus, such separation into physical chemical processes has been questioned [4].

Neville [21] considers as erroneous the view that decalcification of hydrated cement paste through loss of CaOH via efflorescence can lead to loss of cohesion and strength of concrete. He supports this claim by the fact that portland cement is a hydraulic binder that remains strong in water, CaOH has low solubility in water, and there is abundance of submerged structures over prolonged periods of time, such as gravity dams through which there is transport of water without reported decalcification-related damage. However, in the presence of sulfates, the loss of CaOH and resulting lower pH prompts CSH to release CaOH to reestablish equilibrium. Despite the low solubility of CaOH in water described by Neville, the CaOH released in a sulfate medium would immediately serve for the formation of ettringite (Na_2SO_4 or K_2SO_4 attack) or compounds such as $Mg(OH)_2$ ($MgSO_4$ attack). Therefore, the depletion of CaOH is not limited by its concentration in solution as implied by Neville because parallel reactions consuming CaOH catalyze its rapid depletion to the extent that, in extreme cases, CSH itself starts releasing CaOH and losing its binding ability. It is generally in $CaSO_4$ attack that the calcium needed for monosulfate–ettringite conversion can originate entirely from $CaSO_4$ and no decalcification is required. Furthermore, salt deposits in structures subjected to sulfate attack may occur inside the exterior layer of concrete if the drying front moves inward, a situation that does not resemble what is described by Neville for "the many gravity dams that have permeability such that there is some transport of water through the concrete to galleries that collect and remove it".

Moreover, surface scaling observed in the above ground part of concrete structures subjected to groundwater sulfate solutions is at times explained by the progressive lowering of pH that causes decomposition of ettringite into gypsum and other components. The gypsum formation is believed to be responsible for surface scaling. Gypsum does not usually precipitate in the presence of abundant CaOH even when Ca^{2+} and SO_4^{2-} are present, and loss of CaOH through efflorescence can reverse this situation. This is another reason that declining pH through efflorescence or other mechanisms does not only have cosmetic consequences in sulfate environments. Neville recognizes that formation of some salt crystals in the pores of concrete may cause damage; however, he argues that surface efflorescence by itself is not a sign of damage, especially when X-ray analysis (e.g., Fig. 7) demonstrates that it is made of pure Na_2SO_4 with no CaOH leached out. Issues of where salt formation occurs, what distress mechanisms are associated with it, how they relate to observed surface scaling damage, etc., may be the cause of ongoing controversy in this regard.

Neville [22] also states that less permeable concrete will lead to less efflorescence and that the inclusion of pozzolanic materials such as silica fume decreases efflorescence because CaOH is consumed in the pozzolanic reaction and is not available for leaching. This statement is true for CaOH efflorescence but is not true in sulfate environments when

efflorescence is essentially made of sulfate salts. The results of this study show that a w/cm ratio of 0.45 consistently lead to higher efflorescence than a higher w/cm of 0.60. Moreover, silica fume was of no help and indeed made efflorescence worse. Unlike conventional efflorescence in which salts are deposited at the surface after evaporation of water that is moving outward in concrete, sulfate salts are often deposited after capillary rise of sulfate solutions in concrete foundations in contact with sulfate-rich groundwater. With cycling temperature and RH, evaporation occurs and salt deposits appear as a consequence.

It is still curious why an intermediate water/binder (w/b) of 0.45 consistently lead to worse efflorescence deposits in this study than w/cm ratios of 0.30 and 0.60. It may be relevant here to simulate the process of efflorescence by capillary action to the phenomenon of frost heave. Movement of groundwater upward by capillary action under gradually falling temperature creates ice lenses that lift the surface of soil due to the increased volume and continuous supply of groundwater at the frost line. The most prone soils are those that have both high capillarity and relatively high permeability to allow transport of water. Clays that have higher capillarity than silts have lower permeability, whereas fine sands have higher permeability than silts but lower capillarity. The result is that silts tend to be the most prone to frost heave because they provide the adequate capillarity–permeability balance. Similarly, a too low w/cm ratio (0.3) increases capillarity suction due to finer pores, but the total volume of solution transported would be lower due to lower porosity and lower pore connectivity, whereas a too high w/cm results in high porosity but low capillary suction. An intermediate w/cm ratio (0.45) could provide a pessimum compromise, which could explain the observed results.

Yet, no direct evidence of a relationship between Na_2SO_4 efflorescence observed in this study and surface scaling is provided. It is conceivable that, under suitable field conditions, Na_2SO_4 efflorescence can form inside pores; temperature/RH cycling can lead to its repeated conversions between hydrated and unhydrated forms, with associated fatigue and synergistic pressure cycles developing with subsequent salt deposition events. Simultaneously, with carbonation, possible leaching of CaOH, and/or depletion of CaOH in reactions involving sulfates, it is also possible that gypsum deposits form in the same pore space. The generated pressures can add to those from salt crystallization and thenardite/mirabilite conversions. Understanding the mechanisms of the resulting stresses, how surface scaling develops under such conditions, and how mixture design of concrete can be altered to reduce such surface scaling remain open questions that need more focused research.

6. Conclusions

In this study, cement mortars made with plain OPC or OPC incorporating either 8% silica fume, 25% slag, or 25% class F fly ash were made at w/cm of 0.30, 0.45, and 0.60. From the resulting 12 mortar mixtures, standard bars were tested for chemical sulfate attack as per ASTM C1012 by fully submerging the specimens in both 10% Na_2SO_4 and 10% $MgSO_4$ solutions; their expansion and surface deterioration were monitored for up to 9 months of exposure. In addition, mortar cylinders were made from each mixture and tested under partial submersion in both 50-mm-deep 10% Na_2SO_4 and 10% $MgSO_4$ solutions that were maintained at either constant or cycling RH. The development of efflorescence due to salt hydration was monitored. From this work, the following conclusions can be drawn:

- Chemical Na_2SO_4 attack under fully submerged conditions develops essentially through expansion. The higher the w/cm, the higher the expansion. The addition of 8% silica fume was most efficient in reducing expansion followed by 25% slag and 25% class F fly ash, respectively. Surface deterioration of specimens exposed to Na_2SO_4 was not significant.
- Identical mortar bar specimens submerged in $MgSO_4$ exhibited lower expansion than the corresponding values of specimens subjected to Na_2SO_4. Again, the higher the w/cm, the higher the expansion, and mineral additions were effective in reducing expansion in the same order of effectiveness observed in Na_2SO_4. Surface deterioration, likely due to decalcification of CSH, was significant in specimens subjected to $MgSO_4$. Again, the higher the w/cm, the higher the surface deterioration, but silica fume and fly ash did not exhibit any additional benefits in resisting surface deterioration and even lead to worse performance than pure OPC specimens at high w/cm.
- Mortar cylinders partially submerged in a 50-mm-deep 10% $MgSO_4$ solution did not exhibit the formation of surface efflorescence whether the specimens were stored under constant or cycling RH. This is because $MgSO_4$ is not known to have hydrated and anhydrous forms.
- Mortar cylinders partially submerged in a 50-mm-deep 10% Na_2SO_4 solution under constant RH showed the formation of limited efflorescence just above the solution line. However, when specimens were subjected to cycling RH, extensive efflorescence formed on their surface.
- Apparently, an intermediate w/cm of 0.45 provided the most severe conditions for the formation of efflorescence regardless of the binder used in making the mortars. Specimens incorporating silica fume, which is known to refine the pore structure of cement-based materials, were somewhat more vulnerable to formation of efflorescence than the reference OPC specimens.
- X-ray diffraction, SEM imaging, and X-ray energy-dispersive elemental analysis showed that the efflorescence is essentially made of thenardite with traces of mirabilite.
- Further research is needed to understand the distress mechanisms that could be associated with the formation

of such efflorescence and how it is affected by the w/cm, mineral additions, and other mixture parameters of concrete, especially under field conditions.

Acknowledgements

Financial support of the Government of Ontario through the Premier's Research Excellence Award and of the Natural Science and Engineering Research Council of Canada to M. Nehdi are highly appreciated. M. Nehdi also acknowledges funding of the Ontario Innovation Trust and the Canada Foundation for Innovation that allowed creating a state-of-the-art laboratory in which this research was conducted.

References

[1] J. Skalny, J. Pierce, Sulfate attack issues, in: J. Skalny, J. Marchand (Eds.), Material Science of Concrete—Sulfate Attack Mechanisms, American Ceramic Society, Westerville, OH, 1999, pp. 49–64.
[2] M. Santhanam, M.D. Cohen, J. Olek, Sulfate attack research—Whither now? Cem. Concr. Res. 31 (6) (2001) 845–851.
[3] P.K. Mehta, Sulfate attack on concrete: separating myths from reality, Concr. Int. 22 (8) (2000) 57–61.
[4] J. Skalny, J. Marchand, I. Odler, Sulfate attack on concrete, Modern Concrete Technology Series, Spon Press, London, 2002, 217 pp.
[5] P.K. Mehta, Mechanism of sulfate attack on Portland cement concrete—Another look, Cem. Concr. Res. 13 (3) (1983) 401–406.
[6] M.D. Cohen, Theories of expansion in sulfoaluminate type expansive cements: schools of thought, Cem. Concr. Res. 13 (6) (1983) 809–818.
[7] I. Odler, M. Gasser, Mechanism of sulfate expansion in hydrated Portland cement, J. Am. Ceram. Soc. 71 (11) (1988) 1015–1020.
[8] D. Bonen, M.D. Cohen, Magnesium sulfate attack on Portland cement paste: II. Chemical and mineralogical analyses, Cem. Concr. Res. 22 (4) (1992) 707–718.
[9] G.A. Novak, A.A. Colville, Efflorescent mineral assemblages associated with cracked and degraded residential foundations in southern California, Cem. Concr. Res. 19 (1) (1989) 1–6.
[10] C. Rodriguez-Navarro, E. Doehne, E. Sabastian, How does sodium sulfate crystallize? Implications for the decay and testing of building materials, Cem. Concr. Res. 30 (10) (2000) 527–534.
[11] C. Rodriguez-Navarro, E. Doehne, Salt weathering: influence of evaporation rate, supersaturation and crystallization pattern, Earth Surf. Processes Landforms 24 (1999) 191–209.
[12] W.G. Hime, R.A. Martinek, L.A. Backus, S.L. Marusin, Salt hydration distress, Concr. Int. 23 (10) (2001) 43–50.
[13] I.S. Evans, Salt crystallization and rock weathering: a review, Rev. Géomorphol. Dyn. 19 (4) (1970) 153–177.
[14] W.G. Hime, Salt hydration distress—Or is it? Presentation at the ACI Fall Convention, Dallas, 2001.
[15] M.D. Cohen, A. Bentur, Durability of Portland cement—Silica fume pastes in magnesium sulfate and sodium sulfate solutions, ACI Mater. J. 85 (3) (1988) 148–157.
[16] S. Diamond, R.J. Lee, Microstructural alterations associated with sulfate attack in permeable concretes, in: J. Skalny, J. Marchand (Eds.), Material Science of Concrete—Sulfate Attack Mechanisms, American Ceramic Society, Westerville, OH, 1999, pp. 123–174.
[17] H. Haynes, Sulfate attack on concrete: laboratory versus field experiences, Concr. Int. 24 (7) (2002) 64–70.
[18] G.W. Scherer, Crystallization in pores, Cem. Concr. Res. 29 (8) (1999) 1347–1358.
[19] K. Pettifer, P.J. Nixon, Alkali metal sulphate—A factor common to both alkali aggregate reaction and sulphate attack in concrete, Cem. Concr. Res. 10 (2) (1980) 171–173.
[20] H. Haynes, R. O'Neil, P.K. Mehta, Concrete deterioration from physical attack by salts, Concr. Int. 18 (1) (1996) 63–68.
[21] A. Neville, Efflorescence—Surface blemish or internal problems? Part 1: The knowledge, Concr. Int. 24 (8) (2002) 86–90.
[22] A. Neville, Efflorescence—Surface blemish or internal problems? Part 2: Situation in practice, Concr. Int. 24 (9) (2002) 85–88.